ELSEVIER

Journal of Chromatography A, 891 (2000) 129–138

JOURNAL OF CHROMATOGRAPHY A

www.elsevier.com/locate/chroma

Capillary electrophoresis–inductively coupled plasma mass spectrometry interface with minimised dead volume for high separation efficiency

Anders Tangen*, Walter Lund

University of Oslo, Department of Chemistry, P.O. Box 1033, N-0315 Oslo, Norway

Received 1 February 2000; received in revised form 23 May 2000; accepted 23 May 2000

Abstract

A modified microconcentric nebulizer (MCN-100) has been used to construct an improved interface with minimised liquid and gas phase dead volumes for the coupling of capillary electrophoresis (CE) and inductively coupled plasma mass spectrometry (ICP-MS). A plate number of $3.6 \cdot 10^6$ plates m^{-1} has been achieved. This is an order of magnitude better than the results previously reported for CE–ICP-MS. The separation efficiency of the system is demonstrated by the baseline separation of eight rare earth metals within a time span of 14.6 s. The system was used to control the purity of vitamin B_{12} and glutaredoxin 2 from *Escherichia coli*.

Keywords: Capillary electrophoresis–mass spectrometry; Interfaces, CE–MS; Efficiency; Instrumentation; Nebulizing interface; Rare earth metals; Metals

1. Introduction

The coupling of capillary electrophoresis (CE) with inductively coupled plasma mass spectrometry (ICP-MS) and inductively coupled plasma atomic emission spectrometry (ICP-AES) has been reported in a number of papers [1–13]. The combination of the high separation efficiency and the speed of separation achievable by CE with the sensitive element specific capabilities of ICP-MS is a promising instrumental set-up to meet the future challenges of element speciation. Due to the low consumption of sample, CE could be an ideal separation method for expensive samples (e.g., proteins) or in sample-limited situations (e.g., single cells) [14].

Even though a number of papers on CE–ICP-MS and CE–ICP-AES have been published [1–13], the reported separation efficiency is in general relatively low compared to what is theoretically achievable. In most cases the plate numbers are not reported at all. Plate numbers of about 10^6 plates m^{-1} should be obtainable for open capillaries [15], but to the best of our knowledge, no CE–ICP-MS papers report such high numbers. The highest plate number for CE–ICP-MS which has been reported so far is $1.3 \cdot 10^5$ plates m^{-1}, using a direct injection nebulizer (DIN) to interface CE with ICP-MS [2]. However, in a recent paper we demonstrated that there are problems with the grounding of the CE capillary at the tip of a

*Corresponding author. Present address: Amersham Pharmacia Biotech, R&D, Björkgatan 30, SE-75184 Uppsala, Sweden. Fax: +46-18-6121-844.

E-mail address: anders.tangen@eu.apbiotech.com (A. Tangen).

0021-9673/00/$ – see front matter
PII: S0021-9673(00)00617-8

direct injection nebulizer [7], due to interference of the high voltage used for the CE separation with the radio frequency (RF) power supply of the ICP-MS plasma. We found that the CE system should be grounded at the inlet of the nebulizer and a transfer capillary had to be introduced between the end of the electrophoresis capillary and the nebulizer of the ICP-MS.

The aim of the present investigation has been to develop an improved interface for the coupling of CE with ICP-MS. The interface should have a minimum dead volume, to assure high separation efficiency. For on-column UV detection, there is no dead volume, although there are several sources of dispersion [15]. Because ICP-MS is a post-column detection method, some dead volume is inevitable. The challenge is to make the impact of this dead volume as small as possible.

The interface was based on the use of a modified commercial microconcentric nebulizer (MCN-100). In the first part of the present paper, the band broadening effect of the gas and liquid phase dead volumes are studied without CE separation. In particular, the use of the MCN in combination with a spray chamber is evaluated and the effect of the liquid flow-rate is discussed. In the second part of the paper, the use of the MCN for the coupling of CE to ICP-MS is described. It is shown that the MCN-100 should be modified to assure a minimum liquid phase dead volume. The performance of the recommended set-up was studied by analysing a selection of samples.

2. Experimental

2.1. Apparatus

2.1.1. CE–ICP-MS

The recommended CE–ICP-MS set-up is shown in Fig. 1. The CE fused-silica capillary (40 cm×20 μm I.D.×90 μm O.D. if not specified otherwise in the text) was inserted through the nebulizer capillary of a modified MCN-100 (Cetac Technologies, Omaha, NE, USA) Model M-2 microconcentric nebulizer. The original nebulizer capillary (polyimide, 140 μm I.D.) was replaced by a fused-silica capillary (100 μm I.D.×170 μm O.D.). The CE capillary outlet was

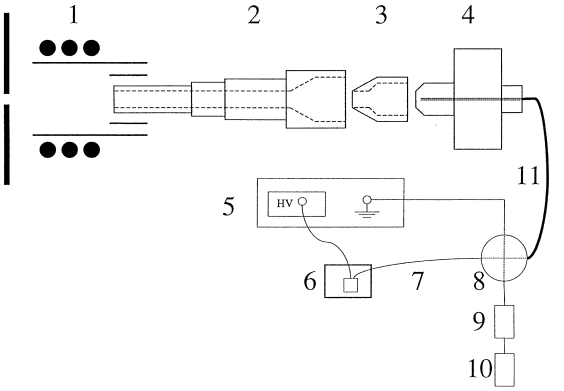

Fig. 1. CE–ICP-MS set-up. The electrical circuit is completed at the nebulizer tip using an extra flow of electrolyte. 1, ICP-MS sampler cone and torch; 2, injector liner; 3, Plexiglas adapter; 4, MCN-100 nebulizer with 100 μm I.D. capillary; 5, high-voltage power supply; 6, CE inlet surrounded by Plexiglas; 7, CE capillary; 8, 1/16 in. cross; 9, HPLC pump; 10, extra electrolyte reservoir; 11, capillary for supply of extra electrolyte to the nebulizer tip.

grounded about 0.8 mm from the tip of the nebulizer capillary by the use of an extra flow of electrolyte supplied by a Shimadzu (Columbia, MD, USA) Model LC-9A pump. The extra flow of electrolyte was connected to a Pt grounding electrode through a 1/16 in. Tefzel cross coupling (Upchurch Scientific, Oak Harbor, WA, USA) and introduced concentrically to the CE outlet (1 in.=2.54 cm). The high-voltage inlet of the CE system was protected by a laboratory-built box made of Plexiglas. Please note that high voltage could cause serious personal injury. Do not touch the CE capillary and the electrodes when the power supply is on. A SpectraPhoresis 100 high-voltage power supply controlled by a SpectraPhoresis 100 modular injector (Thermo Separation Products, CA, USA) was used throughout. No separate cooling system was applied in the CE instrument, but the temperature of the ICP-MS laboratory was regulated by a thermostat and air conditioning system. The separation temperature was monitored for all the runs, and was 22.0°C if not specified otherwise in the text. The nebulizer was coupled directly to the injector liner of the Perkin-Elmer (Norwalk, CT, USA) Sciex Elan 5000 ICP-MS system via a laboratory-made Plexiglas adapter, as shown in Fig. 1. The ICP-MS system was controlled from an IBM PS/2 77 486 DX2 computer equipped

with Elan 5000 (Xenics) software. The ICP-MS operating conditions and data acquisition parameters are given in Table 1.

2.1.2. Direct injection system without CE separation

Experiments without CE separation were carried out. In these experiments a Valco (Houston, TX, USA) Model Cheminert CBW0151 manually operated injection valve with a 20-nl internal loop volume was connected to the ICP-MS system via a transfer capillary and a regular MCN-100 Model M-2 microconcentric nebulizer. The carrier was supplied by a Shimadzu Model LC-9A pump. Before use, the liquid flow-rate delivered by the pump was measured. The nebulizer was coupled directly to the injector liner of the ICP-MS system via a laboratory-made adapter (Plexiglas), or via a regular Scott double pass spray chamber (120-ml internal volume). To produce steady state signals, a Gilson (Villiers, France) peristaltic pump was used for the sample introduction to the MCN-100 nebulizer which was connected to the ICP-MS system via a Scott double pass spray chamber. The liquid flow-rate delivered by the pump was measured before use.

2.2. Reagents and materials

The following analytical quality reagents were used: $Sr(NO_3)_2$ (J.T. Baker, USA), $BaCl_2 \cdot 2H_2O$, HNO_3, K_2CrO_4 and tris(hydroxymethyl)aminomethane (Tris; Merck, Darmstadt, Germany). Spectrascan standards of the rare earth elements, as well as Rh, were supplied by Teknolab (Drøbak, Norway). 4-Methylbenzylamine (UVCAT-1) and tetradecyltrimethylammonium hydroxide (OFM-OH) were obtained from Waters (Milford, MA, USA). α-Hydroxyisobutyric acid (HIBA, ''puriss'' grade) and vitamin B_{12} (>99%) were supplied by Fluka (Buchs, Switzerland). Glutaredoxin 2 was extracted from the bacterium *Escherichia coli* and purified by Alexios Vlamis-Gardikas at the Medical Nobel Institute for Biochemistry, Department of Medical Biochemistry and Biophysics, Karolinska Institute (Stockholm, Sweden). Argon (99.999%) was purchased from AGA (Oslo, Norway). Graphite and vespel ferrules were obtained from Scantec Lab (Partille, Sweden). Fused-silica capillaries were obtained from Composite Metal Services (Worcester, UK).

2.3. Detection limit

The detection limits were estimated with $S/N=3$. The noise was estimated from the baseline of the electropherograms with 20 replicates.

3. Results and discussion

3.1. Introductory experiments without CE separation

3.1.1. The effect of the nebulizer spray chamber

The interface described in the present paper is based on a system with a microconcentric nebulizer. Such a nebulizer is often used in combination with a spray chamber. In order to study the effect of the spray chamber upon transient signals, the direct injection system without CE separation was used (described in Section 2.1.2). This instrumental set-up is easy to operate and it provides short analytical runs (less than 50 s). The injection volume (20 nl) is in reasonable agreement with the injection volumes used in CE. Although the peaks obtained with this system are not as sharp as the peaks obtained with CE, the fundamental band broadening effects caused by liquid and gas phase dead volumes will be the same as those occurring with the set-up shown in Fig. 1. The carrier used was 1.44 m*M* HNO_3 and the flow-rate was 4.4 μl min^{-1}.

The transient ^{103}Rh (100 μg l^{-1}, 20 nl) signals obtained with and without a Scott double pass spray chamber (120 ml internal volume) are shown in Fig. 2. The *x–y* position and the nebulizer gas flow-rate were optimised for both set-ups. Characteristics of the peaks are given in Table 2. It can be seen from Fig. 2 and Table 2 that the spray chamber causes a significant ($P=0.05$) reduction of the peak height, as well as band broadening and a delay (3.7 s) of the peak maximum due to the increased distance from the plasma. In addition, it can be seen from Fig. 2

Table 1
ICP-MS operating parameters

Plasma gas flow-rate	15	l min^{-1}
Auxiliary	1.0	l min^{-1}
Nebulizer (variable)	0.9	l min^{-1}
Forward power	1000	W
Sampler	Pt	Aperture diameter: 1.15 mm
Skimmer	Pt	Aperture diameter: 0.89 mm
Injector liner	Alumina (2.0 mm I.D.)	
Resolution	Normal	
Data acquisition parameters	Direct injection	CE–ICP-MS
Replicate time (ms, variable)	500	10–500
Dwell time (ms, variable)	500	10–500
Scanning mode	Peak hop	Peak hop
Sweeps/reading	1	1
Readings/replicate	1	1
Points/spectral peak	1	1
Isotopes measured	^{103}Rh	^{52}Cr, ^{59}Co, ^{64}Zn, ^{88}Sr, ^{138}Ba, ^{139}La, ^{140}Ce, ^{141}Pr, ^{142}Nd, ^{152}Sm, ^{153}Eu, ^{158}Gd, ^{159}Tb

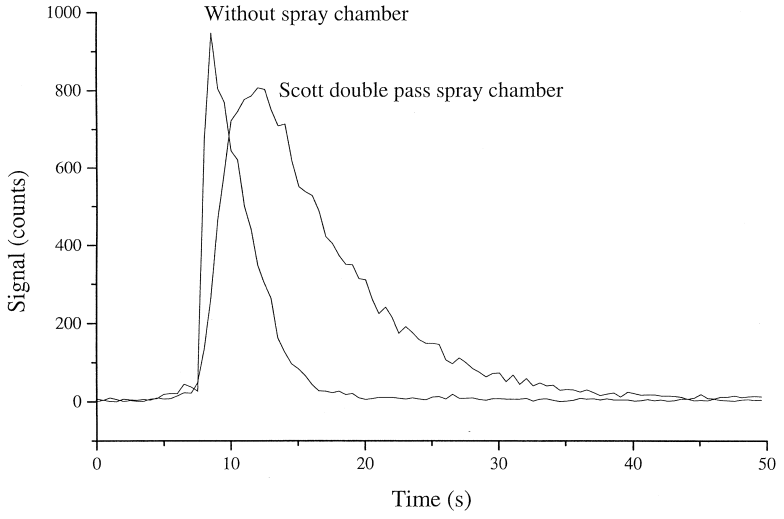

Fig. 2. Signal for ^{103}Rh (20 nl, 100 μg l^{-1}) using a direct injection system with and without a Scott double pass spray chamber.

Table 2
The effect of the spray chamber upon the peak characteristics for Rh (100 μg l^{-1}, 20 nl)

	Peak height±SD (counts)	Peak width±SD[a] (s)	Time±SD[b] (s)	n[c]
Scott spray chamber	783±36	8.9±0.53	12.0±0.45	6
Without spray chamber	874±102	3.8±0.54	8.3±0.27	8

[a] The peak width±SD (standard deviation), measured at half peak height.
[b] The time±SD, measured from injection to peak maximum.
[c] Number of injections.

that the washout time was longer when the spray chamber was used. However, it can also be seen from Table 2 that the precision (SD) is better using the Scott spray chamber. Even so, in order to maintain the high resolution of CE, the spray chamber should be omitted from the instrumental set-up of CE–ICP-MS.

3.1.2. The effect of the liquid phase dead volume

Except for the first paper published on CE–ICP-MS by Olesik et al. [1], all the papers on CE coupled on-line to ICP-MS use an extra flow of electrolyte to complete the electrical circuit at the tip of or at the inlet of the nebulizer. Normally, this will result in a liquid phase dead volume. The impact of this dead volume was studied by varying the inner diameter of the transfer capillary in the direct injection system described in Section 2.1.2. Fused-silica capillaries (length=21 cm) with 15, 50, 100 and 250 μm I.D. were used as transfer capillaries for the connection of the 20-nl injector to the nebulizer. The carrier (1.44 m*M* HNO_3) flow-rate was 4.4 μl min^{-1} and the peak height and width at half height ($w_{1/2}$) for the transient ^{103}Rh (100 μg l^{-1}, 20 nl) signal were measured. It can be seen from Figs. 3 and 4 that the peak height decreases and $w_{1/2}$ increases with an increasing inner diameter of the transfer tubing. Thus, the liquid phase dead volume should be kept as small as possible to maximise sensitivity and minimise band broadening.

3.1.3. The effect of the liquid flow-rate

Because ICP-MS is a mass-sensitive detection method, a steady state signal will increase with increasing liquid flow-rate, provided other parameters are kept constant (aerosol formation, transport efficiency and ICP-MS plasma conditions) [16]. As shown in Fig. 5, the intensity of the steady state ^{103}Rh signal increases rapidly up to about 60 μl min^{-1}. For higher liquid introduction flow-rates, the intensity levels off, probably due to reduced transport efficiency (a Scott double pass spray chamber was used). For the introduction of a small sample plug in a carrier, diffusion and mass transfer resistance processes will influence the peak height and $w_{1/2}$. The band broadening (σ^2) in an open tubular capillary is described by the Golay equation [17]:

$$\sigma^2 = 2DL/u + d_C^2 uL/96D \quad (1)$$

where D is the diffusion coefficient of the analyte, L and d_C are the length and the I.D., respectively, of the capillary and u is the linear flow-rate of the carrier.

The band broadening effect of longitudinal diffusion decreases with increasing linear flow-rate (u) of the carrier, as seen from the first term of Eq. (1). On

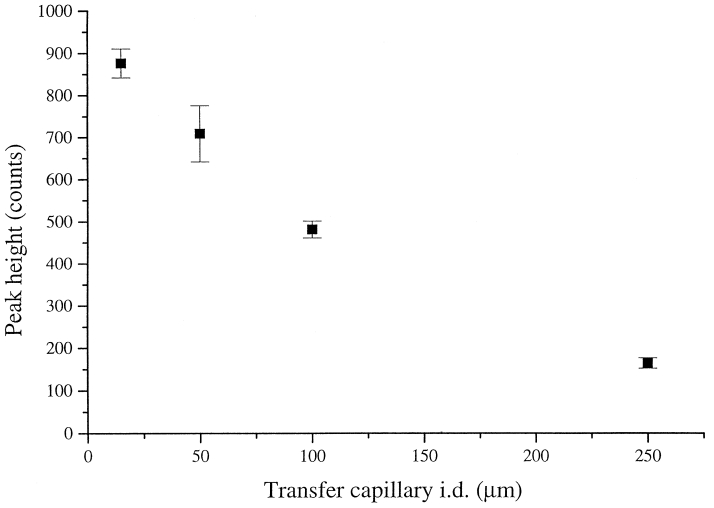

Fig. 3. The peak height (±SD) of ^{103}Rh (20 nl, 100 μg l^{-1}) as a function of the inner diameter of the transfer capillary.

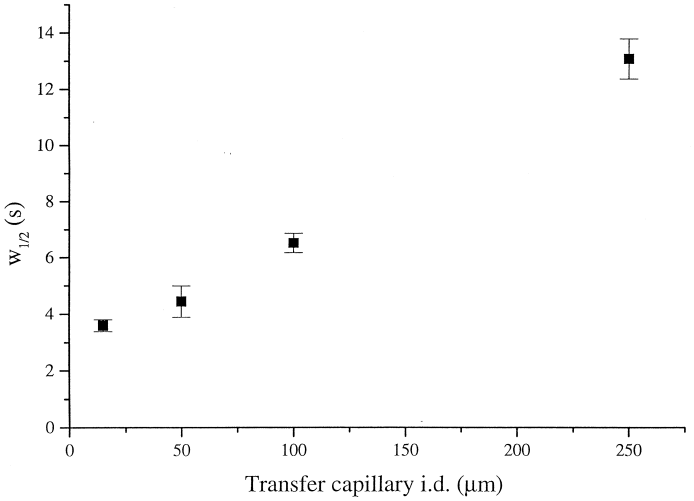

Fig. 4. The width (±SD) at half peak height ($w_{1/2}$) for peaks of ^{103}Rh (20 nl, 100 μg l^{-1}) as a function of the inner diameter of the transfer capillary.

the other hand, the band broadening effect caused by the mass transfer resistance will increase with increasing linear flow-rate of the carrier, as seen from the second term of Eq. (1). The effect of the carrier flow-rate upon $w_{1/2}$ and the peak height was studied using the injection system described in Section 2.1.2. A 20 μm I.D. fused-silica capillary (length = 19 cm) was used to connect the injector to the nebulizer. The carrier (10 m*M* HNO_3) flow-rate was varied between 4.4 and 27 μl min^{-1}. At 22 μl min^{-1}, the plasma started to flicker and at 27 μl min^{-1} it was extinguished. The peak height increased almost linearly with increasing carrier flow-rate. Correspondingly, $w_{1/2}$ decreased.

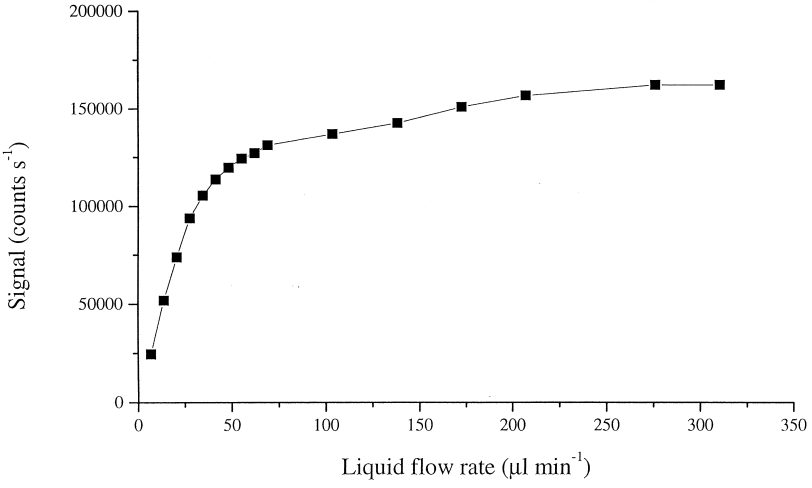

Fig. 5. The intensity of a steady state ^{103}Rh (10 μg l^{-1}) signal as a function of the liquid introductory flow-rate (MCN-100 with Scott double pass spray chamber).

3.2. CE coupled to ICP-MS

3.2.1. A regular MCN-100 nebulizer as interface

For a regular MCN-100 nebulizer, it is possible to position the outlet of a 90 μm O.D. CE capillary inside the nebulizer capillary (3.5 cm×140 μm I.D.). This arrangement provides a low dead volume for the interface, when the electrical circuit is completed at the outlet of the nebulizer. However, this set-up failed to work due to short-circuit problems, probably caused by formation of gas bubbles within the nebulizer capillary. Consequently, the electrical circuit should be completed at the nebulizer inlet. The separation efficiency using this interface was tested on a sample containing a mixture of Ba^{2+}, Ca^{2+}, K^{+}, Mg^{2+}, Na^{+} and Sr^{2+} (1 μg ml^{-1} of each). The CE electrolyte was 6.5 m*M* HIBA and 5.0 m*M* UVCAT-1. The same sample, electrolyte and CE capillary (both I.D. and length) were previously used to test another interface for CE–ICP-MS, based on a laboratory-built direct injection nebulizer [7]. The separation efficiency obtained in the present work with the regular MCN-100 nebulizer as interface was not better than the previously published results [7]. Compared to results obtained using on-column UV detection [18], the resolution was reduced by a factor of five for the CE–ICP-MS system.

Theoretically, the detection limits would improve by the use of a CE capillary with a larger inner diameter than the 20 μm used in the present work. However, inner diameters of 50 and 75 μm were tested with little success; suction effects deterred both migration time reproducibility and the resolution of the separations. The result agrees with the fact that the liquid flow-rate (Q) through a capillary, induced by suction effect, increases with increasing radius (r) of the capillary [19]:

$$Q = \pi r^4 p / 8\eta L \quad (2)$$

where p is the pressure difference through the capillary, η is the viscosity of the liquid and L is the length of the capillary.

3.2.2. A modified MCN-100 nebulizer as interface

In order to reduce the liquid phase dead volume of the CE–ICP-MS set-up, the original nebulizer capillary (140 μm I.D.) of the MCN-100 was replaced by a capillary with 100 μm I.D. Using this modification, it was possible to position the outlet of a 90 μm O.D. CE capillary 0.8 mm from the nebulizer tip without any short-circuit problems. Due to the narrow dimensions used, a HPLC pump had to be used for the introduction of the extra electrolyte. The modified CE–ICP-MS set-up was tested as described in the preceding paragraph. Two carrier flow-rates (8.9 and 13 μl min^{-1}) were tested (ICP-MS dwell time = 10 ms) and, as expected from the earlier experiments, the highest flow-rate gave the best resolution of the Ba and Sr peaks (Table 3), due to the reduction of $w_{1/2}$. Compared to the regular MCN-100 interface, the resolution of the Ba and Sr peaks increased from 1.5 to 5.0, when the thinner capillary was used. Compared to the results obtained with on-column UV detection [18] the resolution was still a factor of 1.5 lower for the CE–ICP-MS system. However, the CE capillary was narrower (20 μm vs. 75 μm) and shorter (40 cm vs. 60 cm) than the one used previously [18], and the analysis time was therefore reduced by a factor of five with the CE–ICP-MS set-up used in the present work. The resolution could

Table 3
Migration time, peak width at half peak height and resolution for Ba and Sr

Flow-rate (μl min^{-1})	n[a]	Migration time±SD[b] (s)		Peak width±SD[c] (s)		Resolution of Ba and Sr, ±SD
		Ba	Sr	Ba	Sr	
8.9	6	62±1.5	64.7±0.61	0.51±0.050	0.67±0.10	2.8±0.37
13	5	63.3±0.25	66.3±0.27	0.36±0.051	0.41±0.093	5.0±1.0

[a] Number of injections.
[b] The migration time±SD (standard deviation), measured at peak maximum, for Ba and Sr, respectively.
[c] The peak width±SD, measured at half peak height, for Ba and Sr, respectively.

easily be improved with the use of a longer CE capillary. The reproducibility of the migration times was 0.4% RSD ($n=5$).

The critical impact of the liquid phase dead volume in a CE–ICP-MS set-up was also demonstrated by measuring the theoretical plate number and the limit of detection (LOD) when the CE outlet was positioned 1 and 4 mm, respectively, from the nebulizer tip. The results and the experimental conditions are shown in Table 4. The theoretical plate numbers increased significantly from $4.5\cdot10^4$ plates m^{-1} to $4\cdot10^5$ plates m^{-1} when the distance of the CE outlet from the nebulizer tip was decreased from 4 to 1 mm, due to the reduction of the liquid phase dead volume. Additionally, the detection limit for Cr^{VI} dropped from 1.8 to 0.8 μg l^{-1} as Cr (unfortunately, the detection limit was still not good enough to quantify the levels of Cr^{VI} found in natural waters).

3.2.3. Applications

The separation speed and efficiency of the current CE–ICP-MS set-up (Fig. 1), based on the modified MCN with a 100 μm I.D. capillary, is demonstrated in Fig. 6a for the separation of eight rare earth elements. Sutton et al. also used a sample of rare earth elements with a similar running electrolyte to test the separation efficiency of a CE–ICP-MS system [5]. Although a separation of the rare earth elements may seem to be unnecessary when ICP-MS is used as detection method, this strategy has previously been used to circumvent isobaric overlaps by the coupling of ion chromatography to ICP-MS [20]. As can be seen from the figure, baseline separation is achieved for all eight elements, within a time span of 14.6 s and a total analysis time of 100 s.

The CE–ICP-MS system, based on the modified MCN (Fig. 1), was also used to look for Co impurities in a vitamin B_{12} (5.5 μg ml^{-1} as Co) sample. The electropherogram is shown in Fig. 6b. No other Co-containing species were detected. A theoretical plate number of $3.6\cdot10^6$ plates m^{-1} was achieved for the protein. Although plate numbers of about 10^6 plates $m^{-1}$are obtainable for open capillaries, the highest plate number for CE–ICP-MS which has been reported so far is $1.3\cdot10^5$ plates m^{-1}, using a DIN to interface CE with ICP-MS [2]. Thus, the plate number obtained in the present work is an order of magnitude higher than the results previously reported for CE–ICP-MS. The limit of detection was 90 μg l^{-1} (Co) using the experimental conditions given in Fig. 6b.

The CE–ICP-MS system was also used to study a protein (glutaredoxin 2 from *E. coli*, $M_r=15\,761.5$ g mol^{-1}) interacting with Zn (1:1), synthesised in a collaborating laboratory. The electropherogram and the experimental conditions are given in Fig. 6c. A detection limit of 0.2 μg l^{-1} (Zn) and a theoretical plate number of $6.5\cdot10^5$ plates m^{-1} was estimated from the signal shown in Fig. 6c. It can be seen from the figure that a minor peak is detected after the main peak. However, due to the basic character (isoelectric point, p$I=9.74$) of the protein, adsorption problems may be severe and definitive conclusions about the purity cannot be given until this problem is overcome.

The use of a short ($L=40$ cm) and narrow (I.D.$=$ 20 μm) CE capillary facilitates the fast separation of high separation efficiency obtained with the CE–ICP-MS set-up presented in this paper. The run time was of the order of 100 s. Apart from the obvious advantage of higher sample throughput, new analytical applications are made possible by the development of faster separation methods. Such examples include the detection of short-lived protein and peptide conformations as well as complexes [21–23].

Table 4
The impact of the liquid phase dead volume upon the plate number and detection limit obtained for Cr^{VI}[a]

Distance from the CE outlet to the nebulizer tip (mm)	Plate number for $Cr^{VI}\pm$SD (plates m^{-1})	LOD (μg l^{-1}, as Cr)	n[b]
1	$4\cdot10^5\pm10^5$	0.8	3
4	$4.5\cdot10^4\pm7.2\cdot10^3$	1.8	4

[a] The experimental conditions were: 53 cm CE capillary, electrokinetic injection (−25 kV, 30 s), separation voltage −25 kV ($T=21.0$°C), ICP-MS dwell time 500 ms. Running electrolyte: 10 m*M* Tris (pH 8.0) and 0.5 m*M* tetradecyltrimethylammonium hydroxide.
[b] Number of injections.

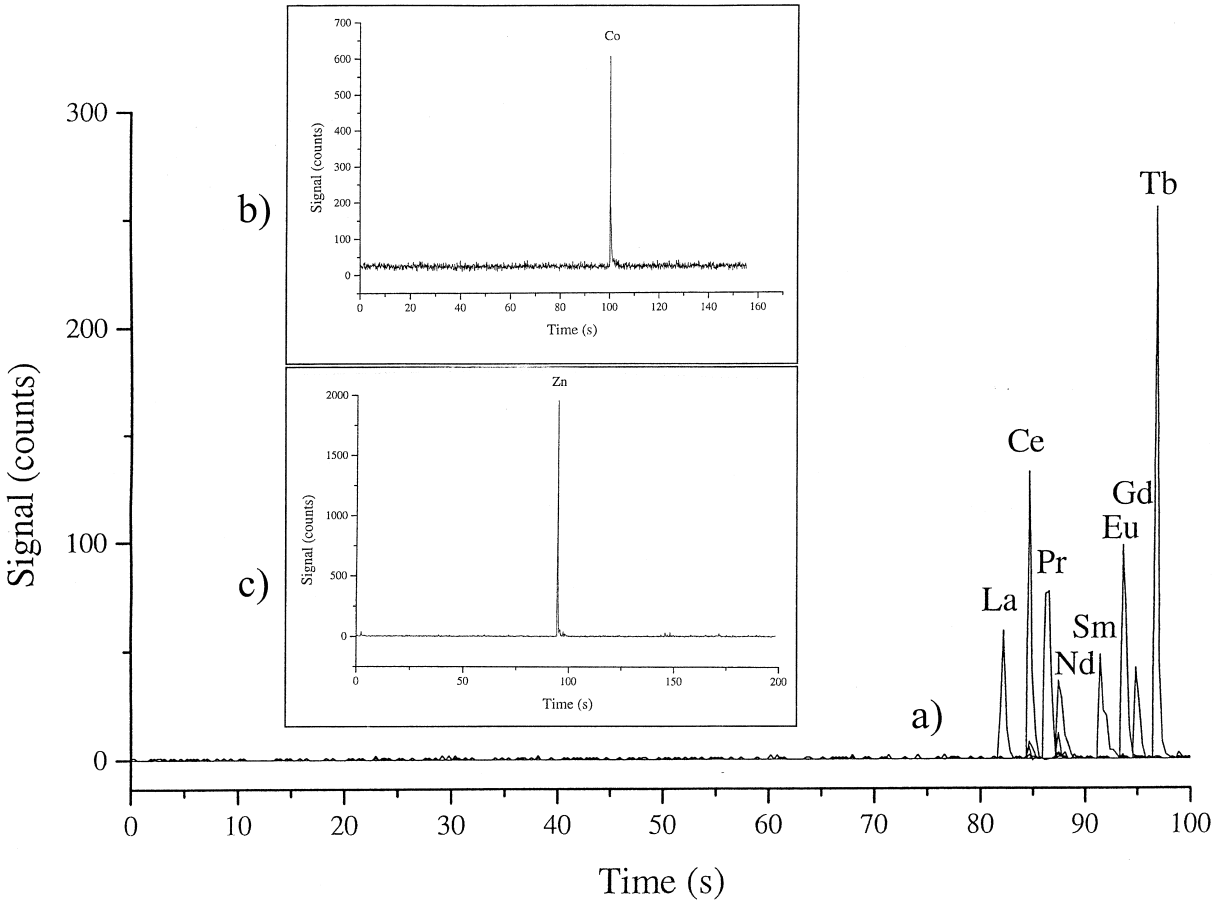

Fig. 6. CE–ICP-MS electropherograms. (a) Sample, 1 μg ml^{-1} of La, Ce, Pr, Nd, Sm, Eu, Gd and Tb; CE electrolyte, 6.5 m*M* HIBA and 5.0 m*M* UVCAT-1 (T=22.0°C); injection, +30 kV (5 s); separation voltage, +30 kV (<1 μA). (b) Sample, vitamin B_{12} (5.5 μg ml^{-1} Co); CE electrolyte, 10 m*M* Tris and 0.5 m*M* tetradecyltrimethylammonium hydroxide (electroosmotic flow modifier, pH 8.0, T=23.0°C); injection, −25 kV (30 s); separation voltage, −25 kV (<1 μA). (c) Sample, glutaredoxin 2 from *E. coli* (110 μg l^{-1} Zn), 1 m*M* Tris, 2 m*M* NaCl and 0.02 m*M* EDTA; CE electrolyte, 20 m*M* Tris (pH 8.0, T=22.0°C); injection, +30 kV (5 s); separation voltage, +30 kV (<1 μA).

With the use of a 8 cm long CE capillary (2 cm effective length×6 μm I.D., 20 kV separation voltage, laser-induced fluorescence detection), Moore Jr. and Jorgenson separated the *cis* and *trans* isomers of the alanine–proline dipeptide within 2.3 s [23]. Correspondingly, by the use of a 8 cm long CE capillary (6 μm I.D.×90 μm O.D.), analysis times less than 10 s should be within reach with the CE–ICP-MS design used in the present work. In the quest for faster separation, even shorter CE capillaries can be applied if the nebulizer is rebuilt with a shorter liquid introduction capillary: the length of the currently used introduction capillary is 3.5 cm. Alternatively, even narrower CE capillaries can be used, facilitating the use of higher field strengths.

In order to obtain well-defined peaks using CE–ICP-MS, the applicable ICP-MS dwell time is limited to a fraction of the peak width. Due to the narrow peaks possibly obtained in miniaturised CE systems, with peak widths of 0.1 s or less, the applicable ICP-MS dwell time is limited. As a result, the detection limits for CE–ICP-MS could be limited by counting statistics. For such CE–ICP-MS instrumentation, quadrupole instruments will probably only be suitable for single ion monitoring, and for single element determination double focusing sector

instruments will provide lower detection limits. For multielement CE–ICP-MS applications, fast scanning time-of-flight (TOF) instruments could be more suitable.

4. Conclusion

An interface with a minimum dead volume has been developed for the coupling of CE and ICP-MS. The interface is based on a commercial microconcentric nebulizer (MCN-100), but the standard nebulizer capillary is replaced by a capillary with 100 μm I.D. The CE–ICP-MS system presented in the present paper is reasonably easy to set-up and use and provides excellent resolution (Fig. 6). A plate number of $3.6 \cdot 10^6$ plates m^{-1} was obtained, which is one order of magnitude higher than the best result previously reported for CE–ICP-MS.

The CE–ICP-MS system does not include a spray chamber. The absence of a spray chamber may have negative effects, such as increased oxide formation. The weakest point of the system is the thin (90 μm O.D.$\times$20 μm I.D.) CE capillary that must be used: scratches, causing the capillary to break, are easily formed through handling of the unusually thin capillary.

The suction effects frequently experienced for CE–ICP-MS were avoided by the use of a narrow CE capillary (20 μm I.D.). Additionally, the use of short CE capillaries with small inner diameters assures faster separations with higher separation efficiency. Fast separations of high separation efficiency in combination with low sample consumption are among the main advantages of CE compared to other separation techniques.

Acknowledgements

The authors thank Rune Bjørnstøl and Roald Østbu at the engineering workshop for valuable technical assistance with the Plexiglas adapter. Alexios Vlamis-Gardikas at the Medical Nobel Institute for Biochemistry, Department of Medical Biochemistry and Biophysics, Karolinska Institute (Stockholm, Sweden) is acknowledged for the supply of glutaredoxin 2.

References

[1] J.W. Olesik, J.A. Kinzer, S.V. Olesik, Anal. Chem. 67 (1995) 1.
[2] Y. Liu, V. Lopez-Avila, J.J. Zhu, D.R. Wiederin, W.F. Beckert, Anal. Chem. 67 (1995) 2020.
[3] G.H. Lu, S.M. Bird, R.M. Barnes, Anal. Chem. 67 (1995) 2949.
[4] B. Michalke, P. Schramel, J. Chromatogr. A 750 (1996) 51.
[5] K.L. Sutton, C. B'Hymer, J.A. Caruso, J. Anal. Atom. Spectrom. 13 (1998) 885.
[6] K.A. Taylor, B.L. Sharp, D.J. Lewis, H.M. Crews, J. Anal. Atom. Spectrom. 13 (1998) 1095.
[7] A. Tangen, W. Lund, B. Josefsson, H. Borg, J. Chromatogr. A 826 (1998) 87.
[8] M. van Holderbeke, Y. Zhao, F. Vanhaecke, L. Moens, R. Dams, P. Sandra, J. Anal. Atom. Spectrom. 14 (1999) 229.
[9] D. Schaumlöffel, A. Prange, Fresenius J. Anal. Chem. 364 (1999) 452.
[10] A. Prange, D. Schaumlöffel, J. Anal. Atom. Spectrom. 14 (1999) 1329.
[11] X.-D. Tian, Z.-X. Zhuang, B. Chen, X.-R. Wang, Atom. Spectrosc. 20 (1999) 127.
[12] V. Majidi, J. Qvarnström, Q. Tu, W. Frech, Y. Thomassen, J. Anal. Atom. Spectrom. 14 (1999) 1933.
[13] S.A. Baker, N.J. MillerIhli, Appl. Spectrosc. 53 (1999) 471.
[14] G. Chen, A.G. Ewing, Crit. Rev. Neurobiol. 11 (1997) 59.
[15] R. Kuhn, S. Hoffstetter-Kuhn, in: Capillary Electrophoresis – Principles and Practice, Springer, Berlin, 1993, p. 37.
[16] A. Tangen, W. Lund, Spectrochim. Acta Part B 54 (1999) 1831.
[17] C.F. Poole, S.K. Poole, in: Chromatography Today, Elsevier, Amsterdam, 1991, p. 21.
[18] A. Tangen, W. Lund, R.B. Frederiksen, J. Chromatogr. A 767 (1997) 311.
[19] L.H.J. Lajunen, in: Spectrochemical Analysis by Atomic Absorption and Emission, Royal Society of Chemistry, Cambridge, 1992, p. 165.
[20] S. Röllin, Z. Kopatjtic, B. Wernli, B. Magyar, J. Chromatogr. A 739 (1996) 139.
[21] R.T. Kennedy, I. German, J.E. Thompson, S.R. Witowski, Chem. Rev. 99 (1999) 3081.
[22] F. Kilar, S. Hjerten, J. Chromatogr. 638 (1993) 269.
[23] A.W. Moore Jr., J.W. Jorgenson, Anal. Chem. 67 (1995) 3464.